Reprinted from **APPLIED OPTICS**, Vol. 13, page 2382, October 1974

Pressure and Stress Dependence of the Refractive Index of Transparent Crystals

Bernard Bendow, Peter D. Gianino, Yet-Ful Tsay, and Shashanka S. Mitra

The pressure derivative of the refractive index *(dn/dP)* and the elastooptic constants *(p_{ij})* in the transparent frequency regime of semiconducting and ionic crystals are investigated theoretically. The electronic contribution to *dn/dP* of semiconductors is obtained by carrying out pseudopotential calculations of the band structure as a function of hydrostatic pressure, and the results compared with experiment. The lattice contribution to *dn/dP* is obtained by relating *dn/dP* to changes in the effective ionic charge and the phonon spectrum as functions of pressure. As for the p_{ij}, we perform a detailed application of the theory of Humphreys and Maradudin to calculate these for a variety of cubic crystals as functions of frequency in the transparent regime. The parameters required in the calculation are determined from improved prescriptions, which relate various microscopic functions to experimental data on the pressure dependence of phonon frequencies. The theoretical results are checked employing a relation between *dn/dP* and the p_{ij}. Overall, one finds that frequency dispersion is most important for the ionic materials and is generally negligible for the more highly covalent materials.

I. Introduction

Photoelasticity, i.e., the change in refractive index induced by stress, has long been a subject of considerable interest in the optics of crystals.[1] Recent attention to photoelastic effects has also been stimulated by the recognition that they contribute to distortion of high power laser beams, thereby compromising the optical performance of high power laser systems and their associated applications.[2] The pressure dependence of the refractive index *(n)*, for example, contributes to pressure-induced distortion[3] and is embodied by the derivative *dn/dP*. The stress dependence of *n* is relevant to the optics of transparent materials because it is associated with a variety of unacceptable distortion effects on the transmission of laser beams, such as interference and multiple refraction.[1] In high power applications, thermally induced stresses contribute to the thermal lensing of spatially nonuniform laser beams and the concomitant degradation of the transmitted beam.[4] Whether the stresses are external or internal, the optical performance of laser windows may be severely compromised by the resultant distortion effects. The extent of the latter effects may be predicted if the elastooptic constants p_{ijkl} are known; for example, one requires them to determine the effective temperature derivative of *n*, which measures the potential for optical distortion in laser window materials.[4] The elastooptic coefficients are defined as[5]

$$\Delta(1/n^2)_{ij} = p_{ijkl}\tau_{kl}, \tag{1}$$

where τ is the strain tensor. Stress-optic coefficients may be defined analogously by expressing strain in terms of stress. For the present purposes we are interested primarily in cubic diatomic crystals where just three independent coefficients remain; these are p_{11}, p_{12}, and p_{44} in the standard contracted notation.[5]

The objective of the present work is to predict both the magnitude and the frequency dependence of *dn/dP* and the *p*s throughout the transparent regime of crystals. Our primary interest will be in the ir region, where high power laser applications have stimulated much attention recently.[2] A pressure-dependent pseudopotential method is applied to calculate the electronic contribution to *dn/dP* of semiconductors, while a phenomenological method is introduced to obtain the corresponding quantity for ionic crystals. The lattice contribution to *dn/dP* is calculated from a combination of experimental and phenomenological prescriptions, which determine the pressure derivatives of the lattice resonance frequency ω_0 and its associated transverse effective charge e_T^*. The lattice contributions to the *p*s are obtained from the

B. Bendow and P. D. Gianino are with the Solid State Sciences Laboratory, Air Force Cambridge Research Laboratories (AFSC), Bedford, Massachusetts 01730; the other authors are with the Department of Electrical Engineering, University of Rhode Island, Kingston, Rhode Island 02881.

Received 1 March 1974.

theory of Humphreys and Maradudin[6] (HM). However, it is pointed out that the models employed by HM are inadequate, and these are improved by relating microscopic functions in the theory to experimentally available data on pressure dependence of ω_0 and e_T*. Computations are carried out for a wide variety of cubic crystals of interest, both with HM's and the present prescriptions, and the results compared.[7]

II. Oscillator Model for Refraction

For many purposes the refraction of a solid may be viewed as associated with a number of discrete oscillators of frequencies ω_i and strengths g_i. In particular, in the transparent regime of laser window materials lying in between the fundamental lattice resonance (ω_0) and the energy gap (ω_g), a simplified model consisting of just a single oscillator each for the lattice and the electrons is generally sufficient.[8] The susceptibility χ due to an oscillator at a transparency frequency ω may be expressed as[9]

$$\chi_i(\omega) = g_i(\omega_i^2 - \omega^2)^{-1}. \quad (2)$$

It is also conventional to introduce an effective plasma frequency associated with ω_i, defined as $\omega_{pi}^2 = 4\pi g_i$. The refractive index n is given by[9]

$$n^2(\omega) = 1 + 4\pi \sum_i \chi_i(\omega). \quad (3)$$

This simple equation is a useful starting point for investigating the effects of perturbations on n. The change in n associated with the parameter x follows directly as

$$\frac{dn}{dx} = \frac{2\pi}{n} \sum_i \left[\frac{1}{g_i} \frac{dg_i}{dx} - \frac{d\omega_i^2}{dx} \frac{1}{\omega_i^2 - \omega^2} \right] \chi_i(\omega). \quad (4)$$

Thus one requires the changes induced in g_i and ω_i due to changes in the parameter x to evaluate dn/dx. In the present paper we are interested specifically in the case in which x is either the pressure P, or a given strain component τ_j. In the pressure case, for example, we require $d\omega_0/dP$, $d\omega_g/dP$, $d\omega_{pe}^2/dP$, and $d\omega_{pL}^2/dP$, where e and L stand for electronic and lattice, respectively.

It is useful to distinguish the density dependence in g_i by writing

$$\omega_{pi}^2 = 4\pi N_i e_i^{*2}/m_i, \quad (5)$$

where N_i is the number of oscillators per unit volume, e_i* their effective charge, and m_i their effective mass. In evaluating dn/dx, dg_i/dx is generally best expressed in terms of dN_i/dx and de_i^*/dx, the quantities that possess the greater physical significance.

III. Electronic Contribution to dn/dP in Semiconductors

In this section we calculate the electronic contribution to dn/dP in semiconductors, employing a pseudopotential band structure method.[10] Previously, Camphausen *et al.*[11] (CCP) calculated dn/dP by employing an extension of Van Vechten's dielectric theory.[12] The objective here will be to carry out calculations that are closer to first principles, for dn/dP of diamond and zincblende semiconductors, by employing an empirical pseudopotential band-structure approach.[10] We here sketch the method and present the results. Details will be given in a parallel publication.[13] Pressure dependent band-structure calculations have also been carried out recently by Melz,[14] employing the model pseudopotential method, but the **k**s which will be of interest here were not included.

Adopting an approach similar to that employed by Tsay *et al.*[8] for calculating the temperature dependence of n, one takes, for $\omega \ll \omega_g$,

$$\epsilon_\infty = n^2 = 1 + \omega_p^2/\omega_g^2, \quad (6)$$

where ω_p is the effective electronic plasma frequency and ω_g the effective bandgap, taken here simply as the gap at the point $\mathbf{k} = 2\pi a^{-1}$ (½, ½, 0) of the Brillouin zone. The latter assignment is motivated by a variety of recent experimental and theoretical work,[15] which suggest that the strongest peak in the optical spectra of the crystals of interest here is from transitions near this point. We here assume that the electronic e* is independent of pressure; then using Eq. (6) and accounting for the density dependence of ω_p^2, one obtains

$$n^{-1}dn/dP = \frac{1}{2}(1 - n^{-2})(K - 2\omega_g^{-1}d\omega_g/dP), \quad (7)$$

where K is the isothermal compressibility. The latter is known reasonably accurately for most crystals. Thus, the central task becomes the evaluation of $d\omega_g/dP$, which we carry out here employing the pseudopotential band-structure method.

We adopt the following assumptions and procedures in calculating ω_g as a function of pressure: The principal effects of pressure on the band structure are considered to be accounted for by allowing the lattice constant a to be a function of pressure. Values of $a(P)$ are calculated starting from atmospheric values, by employing a K that is assumed independent of pressure. The pseudopotential form factors appropriate for small changes in a are calculated within the rigid-ion approximation,[16] starting from atmospheric pressure values taken from Cohen and Bergstresser.[17]

The calculated variation of ω_g with P is illustrated for some typical cases in Fig. 1. We note the linear dependence of ω_g on P up to 20 kbar. The final calculated values of $d\omega_g/dP$ and dn/dP are listed in Table I, alongside the calculated values of CCP and available experimental data.[18] Our values for dn/dP are observed to be similar to those of CCP for diamond-type and III–V crystals, except for the case of GaP. The origin of the positive value of dn/dP for GaP is an unusually small value of $d\omega_g/dP$ calculated for this crystal. In the case of II–VIs, however, our results differ substantially from those of CCP. The

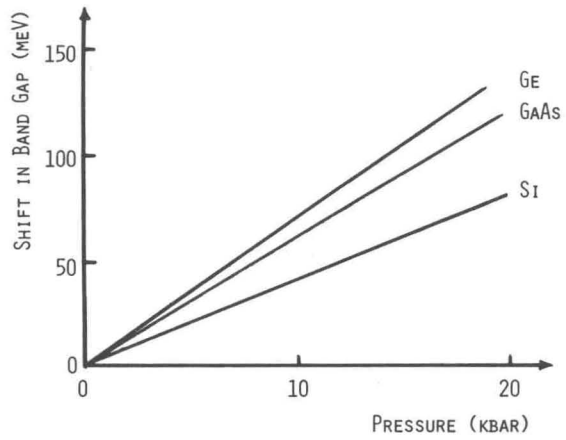

Fig. 1. Shift in bandgap $\Delta\omega_g$ vs pressure for some semiconductors.

$$\frac{dn_e^2(\omega)}{dP} = \chi_e(\omega)\left[K - \frac{2}{\omega_g}\frac{d\omega_g}{dP}(1 - \omega^2/\omega_g^2)^{-1}\right]. \quad (8)$$

χ_e requires ω_p^2, which is available in a wide variety of places, such as Ref. 19; the remaining parameters are the same as required in Eq. (7). The frequency dependence for $\omega \to \omega_g$ is very similar to that for $\omega \to \omega_0$, with the latter the primary region of interest for this work. Explicit calculations of dn/dP vs ω will thus be restricted to the ir regime (See Sec. V).

IV. Electronic Contribution to dn/dP of Ionic Crystals

Pseudopotential and related methods of calculation of band shifts with pressure or changes in temperature do not appear to have yielded satisfactory results as yet for ionic crystals.[8] For this reason, it is preferable to adopt a more phenomenological approach to the prediction of dn/dP for this case. We may again use Eq. (6) as a starting point, whence calculation of $d\omega_g/dP$ becomes the central objective. We here choose to calculate $d\omega_g/dP$ starting from the Phillips-Van Vechten prescription,[12] namely, the relation

$$\omega_g^2 = h^2 + C^2, \quad (9)$$

$$h \cong r^{-2.5}, \quad (10)$$

where h and C are the homopolar and heteropolar gap, respectively, and r is the equilibrium nearest neighbor distance. From Eqs. (6), (9), and (10), one can easily obtain

$$\frac{dn}{dP} = \frac{\epsilon_\infty - 1}{3\sqrt{\epsilon_\infty}}\left[1.5 - 2.5(1 - f) + f\frac{r}{C}\frac{\partial C}{\partial r}\right]K, \quad (11)$$

where $f = C^2/\omega_g^2$, is the ionicity[20] in Phillips' scale. Theoretical calculation of $(r/C)\,\partial C/\partial r$ turns out to be rather difficult. However, after inspecting experimental data of dn/dP for various ionic crystals, Van

Table I. Electronic dn/dP of Semiconductors

Crystal	K (10^{-6}/bar)	ω_g (eV) (Ref. 12)	ϵ_∞	$d\omega_g/dP$ (10^{-6} eV/bar)	$(1/n)(dn/dP)(10^{-6}$/bar) This work	CCP	Experiment (Ref. 18)
Si	1.02	4.8	12.0	4.1	−0.31	-0.3 ± 0.05	−0.3
Ge	1.33	4.3	16.0	7.0	−0.89	-1.0 ± 0.2	−0.7 to −1.0
GaSb	1.71	4.1	14.4	9.1	−1.23	-0.8 ± 0.2	—
GaAs	1.34	5.2	10.9	5.9	−0.44	-0.5 ± 0.2	-0.7 ± 0.1
InSb	2.20	3.7	15.7	9.2	−1.30	-1.1 ± 0.2	—
InAs	1.72	4.6	12.3	5.9	−0.39	-0.7 ± 0.2	—
GaP	1.13	5.8	8.5	2.0	+0.20	-0.3 ± 0.2	—
AlSb	1.69	4.7	10.2	5.7	−0.33	-0.5 ± 0.2	—
InP	1.38	5.2	9.6	6.2	−0.45	-0.4 ± 0.2	—
ZnS	1.39	7.8	5.0	1.9	+0.36	0.05 ± 0.1	−0.1
ZnTe	2.00	5.8	7.3	4.9	+0.14	0.01 ± 0.1	—
ZnSe	1.70	7.4	6.1	3.5	+0.32	0.07 ± 0.1	—
CdTe	2.36	5.5	7.1	3.8	+0.53	0.1 ± 0.1	—

present calculated values display good agreement with experiment for Si and Ge, fair for GaAs, and poor for ZnS. Unfortunately, adequate data are not available for a more thorough comparison of theory with experiment. Nevertheless, some comments are in order regarding our results for the II–VIs: On the one hand, the trend to more positive values for the II–VIs is in agreement with the larger values of K and ω_g associated with increasingly ionic materials (dn/dP is large and positive for highly ionic materials such as alkali halides). However, an uncertainty in our calculation for II–VIs appears to be the stronger variation in $d\omega_g/dP$ for different points in the zone for these crystals, not accounted for by the simple assignments discussed above. Nevertheless, the empirical pseudopotential method appears to be a very promising fundamental method for the calculation of dn/dP.

Turning to the frequency dependence in the electronic regime ($\omega_0 \ll \omega < \omega_g$), this may be calculated directly from Eq. (4) with $de^*/dP = 0$, the present approximation, whence

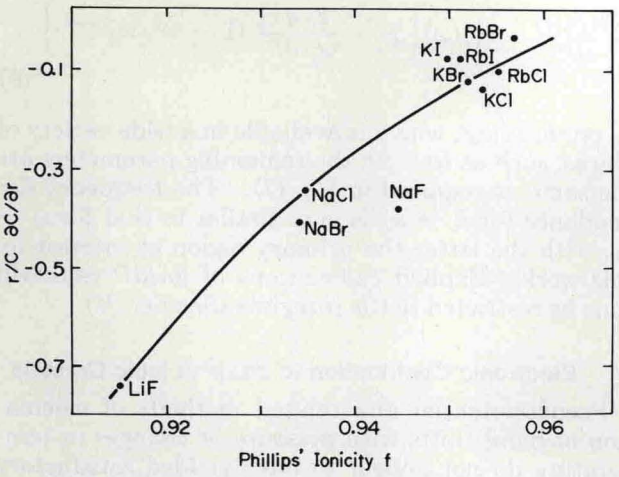

Fig. 2. $(r/C)\ \partial C/\partial r$ vs f for ionic crystals; f from Ref. 20. Data are calculated values deduced from experimental data on $\partial n/\partial V$ of G. R. Barsch and B. N. Achar, Phys. Stat. Sol. **35**, 881 (1969).

Vechten[12] arrived at the interesting conclusion that $(r/C)\ \partial C/\partial r \to 0$ in the perfectly ionic limit when $f \to 1$. He further pointed out that the above conclusion could be anticipated from the fact that the crystalline equilibrium distance should be such as to minimize the cohesive energy of the crystal. In the ionic limit, $f \to 1$, the Madelung energy makes the whole contribution to the cohesive energy, and the latter condition is equivalent to requiring C to be a maximum. Since $f = 1$ is never reached in real cases, we can always expect small deviations from the condition $\partial C/\partial r = 0$.

The above discussion suggests that a meaningful parameterization is accomplished by assuming that $\partial C/\partial r$ is a function of ionicity only, which is equal to zero when $f = 1$. Letting

$$\frac{r}{C}\frac{\partial C}{\partial r} = g(f), \tag{12a}$$

we then expand $g(f)$ about $f = 1$:

$$g(f) = \frac{dg}{df}(f-1) + \frac{1}{2}\frac{d^2g}{df^2}(f-1)^2 + \ldots, \tag{12b}$$

where we have assumed $g(1) = 0$. It is expected that the higher order terms can be neglected because for most ionic crystals $f \geq 0.9$.

The above argument can be put to the test by plotting experimental data of $\partial C/\partial r$ against f and seeing if these data can be fitted reasonably well by a formula of the form

$$a(1-f) + b(1-f)^2\ . \tag{13}$$

Such a plot is shown in Fig. 2, where the solid line is obtained using only the experimental data of LiF, NaCl, and KBr, which are thought to be most reliable. Indeed, the dependence of $\partial C/\partial r$ on f is well represented by Eq. (13) with $a \approx 6.034$, $b \approx -173.8$. In Table II we have used these values along with Eq. (6) to calculate dn/dP for a large number of ionic crystals. Where experimental data exist the comparison is excellent. Furthermore, the correct sign of dn/dP for MgO is predicted, although its predicted magnitude is only within a factor of 2 or so. However, this is because Eq. (13) is expected to hold true for $f \cong 1$. For less ionic materials such as MgO, where $f = 0.84$, we probably need to retain more terms in the expansion of $\partial C/\partial r$.

V. Lattice Contribution to dn/dP

The origin of the wavelength dependence of dn/dP in the transparent regime of interest for ir applications is the pressure dependence of the lattice resonance of the material. Using the formalism of Sec. II, one easily finds in this regime

$$\frac{dn}{dP} = \frac{n_e}{n}\left(\frac{dn}{dP}\right)_e + \frac{1}{n}\left\{\frac{\epsilon_0 - \epsilon_\infty}{1 - \dfrac{\omega^2}{\omega_0^2}}\left[\frac{1}{2}K + \frac{1}{e_T^*}\frac{de_T^*}{dP} - \frac{(1/\omega_0)(d\omega_0/dP)}{1 - (\omega^2/\omega_0^2)}\right]\right\}, \tag{14}$$

where we have used the relation $\omega_{pL}^2 = (\epsilon_0 - \epsilon_\infty)\omega_0^2$ for the lattice resonance, and ϵ_0 is the low frequency dielectric constant.[21] Of the parameters appearing above, $(dn/dP)_e$ has been calculated in Secs. III and IV, and K, ϵ_0, and ϵ_∞ are readily available; it remains to determine just de_T^*/dP and $d\omega_0/dP$. $d\omega_0/dP$ is related to the Gruneisen parameter γ_{TO} by[22]

$$(1/\omega_0)(d\omega_0/dP) = K\,\gamma_{TO}. \tag{15}$$

Experimental values of $d\omega_0/dP$ are available for a variety of crystals. If the interionic potential and re-

Table II. Electronic dn/dP of Ionic Crystals

Crystal	α (10^{-5}/K)	K^{-1} (10^{12} dyne/cm^2)	f[a]	dn/dP (10^{-12} cm^2/dyne) Expt.	Calc.
LiF	3.7	0.67	0.915	0.198	0.197
NaF	3.6	0.465	0.946	0.398	0.465
NaCl	4.4	0.24	0.935	1.17	1.178
NaBr	4.2	0.2	0.934	1.57	1.65
KCl	3.6	0.174	0.953	1.82	1.87
KBr	4.3	0.148	0.952	2.44	2.46
KI	4.26	0.117	0.95	3.85	3.68
MgO	1.1	1.693	0.84	−0.158	−0.416
RbCl	3.5	0.156	0.955	2.24	2.26
RbBr	3.6	0.130	0.957	3.0	2.93
RbI	3.5	0.106	0.951	4.25	4.10
LiCl	4.3	0.298	0.903	—	0.358
LiBr	4.9	0.238	0.899	—	0.347
LiI	5.8	0.171	0.89	—	−0.156
NaI	4.5	0.151	0.927	—	2.14
KF	3.5	0.305	0.955	—	0.585
RbF	3.5	0.262	0.96	—	1.13

[a] From Ref. 20.

sulting cohesive energy per cell are known, then one can obtain a theoretical expression for γ as well. This procedure is discussed in some detail for various crystal models in Ref. 22. We here quote the results for just the Born-Mayer potential:

$$v(r) = \pm (e^2/r) + \lambda \exp(-r/\rho), \tag{16}$$

where e is the electronic charge. For the TO and longitudinal optical (LO) modes one obtains

$$\gamma_{TO} = (f_1/f_2 - f_3)/(f_1 - 2f_3),$$
$$\gamma_{LO} = (f_1/f_2 + 2f_3)/(f_1 + 4f_3), \tag{17}$$
$$f_1 \equiv \frac{\sigma - 2}{3}\frac{\alpha e^2}{r_0^3}, \quad f_2 \equiv \frac{\sigma^2 - 2\sigma - 2}{6(\sigma - 2)}, \quad f_3 \equiv \frac{\pi}{3}\frac{e^2}{r_0^3},$$
$$\sigma \equiv r_0/\rho,$$

where α is the Madelung constant and r_0 the equilibrium nearest neighbor distance.

The quantity de_T^*/dP is not unambiguously available from experiment, and we therefore employ the relations[21]

$$\epsilon_0 - \epsilon_\infty = 4\pi e_T^{*2} N/\mu\omega_0^2, \tag{18}$$
$$\omega_{LO}^2/\omega_{TO}^2 = \epsilon_0/\epsilon_\infty$$

as the starting point of a calculation of de_T^*/dP. One obtains directly

$$\frac{1}{e_T^*}\frac{de_T^*}{dP} = \frac{1}{n}\left(\frac{dn}{dP}\right)_e + K\left[\frac{\epsilon_0}{\epsilon_0 - \epsilon_\infty}\gamma_{LO} - \frac{\epsilon_\infty}{\epsilon_0 - \epsilon_\infty}\gamma_{TO} - \frac{1}{2}\right], \tag{19}$$

which may be used in conjunction with the previous expressions for $(dn/dP)_e$, γ_{LO}, and γ_{TO}.

Values of relevant parameters entering the computation of dn/dP are listed in Tables III and IV. Calculated curves of dn/dP vs wavelength are illustrated for exemplary crystals in Fig. 3. Values of dn/dP at selected wavelengths of interest are compared in Table V. It is evident that the dispersion in semiconductors is much smaller than that in ionic crystals; a well expected consequence of the smallness of the lattice polarizability relative to the electronic in these crystals $[(\epsilon_0 - \epsilon_\infty)/\epsilon_\infty \ll 1]$.

VI. Photoelasticity—Theoretical Considerations

A. *Formal Expressions for Elastooptic Coefficients*

The aim of the present section is to obtain theoretical predictions of the elastooptic constants of ir transmitting materials as functions of frequency.[7] Frequency dependence is especially important because very little data are available in the ir, where such measurements are especially difficult, yet the effects of dispersion may be sizable. We will here focus attention on two types of crystal, ionic crystals of the rocksalt (RS) type and semiconductors of the zinc

Table III. Parameters for Calculation of Lattice dn/dP in Ionic Crystals[a]

Material	ϵ_0	ϵ_∞	ϵ_S^*	e_T^*	$\omega_0(\text{cm}^{-1})$	$r_0(\text{Å})$	K (10^{-6}/bar)	$-\frac{1}{e_T^*}\frac{de_T^*}{dP}$ (10^{-6}/bar)	$\frac{1}{\omega_0}\frac{d\omega_0}{dP}$ (10^{-6}/bar)
LiF	8.81	1.9	0.87	1.13	306	2.01	1.49	0.29	3.98
LiCl	12.0	2.7	0.73	1.14	191	2.57	3.36	0.26	8.23
LiBr	13.2	3.2	0.68	1.18	159	2.75	4.20	0.42	10.25
NaF	5.1	1.7	0.93	1.15	244	2.31	2.15	0.65	5.25
NaCl	5.9	2.25	0.74	1.05	164	2.81	4.17	1.29	10.18
NaBr	6.4	2.6	0.70	1.07	134	2.98	5.02	1.70	12.35
NaI	6.6	2.91	0.71	1.16	117	3.23	6.62	3.05	16.42
KF	5.5	1.5	0.88	1.03	190	2.67	3.28	−0.19	7.94
KCl	4.85	2.13	0.81	1.11	142	3.14	5.75	2.16	14.43
KBr	4.9	2.3	0.76	1.09	113	3.29	6.76	3.2	17.04
KI	5.1	2.7	0.71	1.11	101	3.53	8.85	6.7	22.66
RbF	6.5	1.9	0.95	1.23	156	2.82	3.82	−0.45	9.47
RbCl	4.90	2.2	0.84	1.18	116	3.27	6.4	2.01	16.38
RbBr	4.90	2.3	0.84	1.20	88	3.43	7.7	3.1	19.71
RbI	5.50	2.6	0.75	1.15	75	3.66	9.45	3.4	24.57
MgO	9.64	3.0	1.76	2.94	400	2.10	0.596	−0.29	1.95
CaO	11.1	3.33	1.76	3.10	295	2.41	1.00	−1.05	3.52
AgCl	12.3	4.0	0.71	1.42	103	2.78	2.45	−0.25	7.48
AgBr	13.1	4.6	0.70	1.54	80	2.89	2.47	−0.13	7.83

[a] de_T^*/dP and $d\omega_0/dP$ calculated from theoretical values of γ as described in the text. Existing experimental values generally agree with the theory within ~20% [see, e.g., J. R. Ferraro, S. S. Mitra, and A. Quattrochi, J. Appl. Phys. 42, 3677 (1971)].

Table IV. Parameters for Calculation of Lattice dn/dP in Semiconductors

Material	ϵ_0	ϵ_∞	$\epsilon_S{}^*$	$\epsilon_T{}^*$	$\omega_0(\mathrm{cm}^{-1})$	r_0(Å)	K (10^{-6}/bar)	$\frac{1}{e_T{}^*}\frac{de_T{}^*}{dP}$ (10^{-6}/bar)	$\frac{1}{\omega_0}\frac{d\omega_0}{dP}$ (10^{-6}/bar)
GaP	10.18	8.46	0.59	2.04	367	2.36	1.13	0.41	1.18
GaAs	12.9	10.9	0.50	2.16	269	2.45	1.34	−0.16	1.74
GaSb	15.69	14.44	0.33	2.15	230	2.65	1.77	0.07	2.12
AlSb	11.21	9.88	0.48	2.30	319	2.66	1.69	0.35	2.03
ZnS	8.3	5.0	0.92	2.15	271	2.35	1.39	−0.99	2.78
ZnSe	9.2	6.1	0.75	2.03	207	2.46	1.7	−1.25	2.81
ZnTe	10.38	7.8	0.62	2.00	177	2.63	2.0	−2.61	3.12
CdTe	10.2	7.1	0.77	2.35	141	2.81	2.36	—	—

[a] $de_T{}^*/dP$ and $d\omega_0/dP$ deduced from experimental values of γ from Raman spectra under hydrostatic pressure: GaP, ZnS, ZnSe, and ZnTe from S. S. Mitra, O. Brafman, W. B. Daniels, and R. K. Crawford, Phys. Rev. **168**, 942(1969) others from C. J. Buchenauer, F. Cerdeira, and M. Cardona, in *Light Scattering Spectra of Solids*, M. Balkanski, Ed. (Flammarion, Paris, France, 1971).

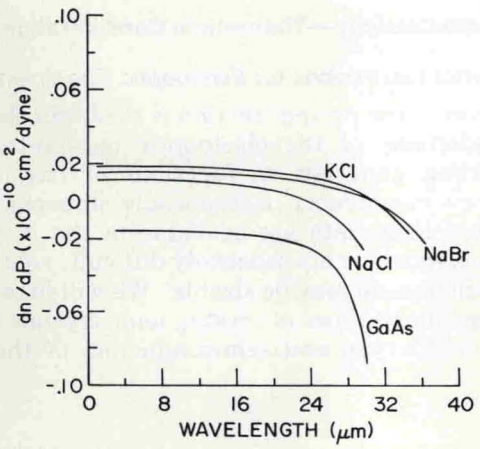

Fig. 3. Infrared wavelength (μm) dependence of dn/dP (cm²/dyne) for typical crystals.

Table V dn/dP at Selected Wavelengths

Crystal	$dn/dP \times 10^{12}$ (cm²/dyne) Electronic Values	3.9 μm	10.6 μm
LiF	0.198	0.166	−0.457
LiCl	0.358	0.315	−0.076
LiBr	0.347	0.312	0.020
NaF	0.398	0.391	0.267
NaCl	1.170	1.166	1.114
NaBr	1.570	1.567	1.541
NaI	2.140	2.142	2.144
KF	0.585	0.554	0.303
KCl	1.820	1.819	1.801
KBr	2.440	2.442	2.450
KI	3.850	3.858	3.904
RbCl	2.240	2.238	2.220
RbBr	3.000	3.001	3.001
RbI	4.250	4.250	4.248
ZnS	0.872	0.880	0.905
ZnSe	0.914	0.919	0.943
GaP	0.582	0.571	0.466
GaAs	−1.585	−1.590	−1.634

blende (ZB) type. The principal source of photoelasticity in the ir for these materials is the change of crystalline vibrational frequencies and polarizabilities induced by stress fields. We will here employ the theory of HM to determine the latter effects. We note that for the cubic diatomic crystals investigated here, we have the relation[5]

$$n^3K(p_{11} + 2p_{12}) = 6dn/dP, \tag{20}$$

which will play a central role in the considerations to follow. At this point we can utilize the above relation to estimate the size of the ps. With typical values of $K \sim 10^{-6}$/bar and $n^{-1}/dn/dP \sim \frac{1}{2} \times 10^{-6}$/bar, one obtains

$$p_{11} + 2p_{12} \sim 3/n^2, \qquad p_{ij} \sim 1/n^2. \tag{21}$$

Thus, the magnitude of the p_{ij} is roughly on the order of the inverse dielectric constant, typically about 0.1 to 0.3.

We now employ the formalism of Sec. II to yield a qualitative description of the frequency dependence of the ps. Taking

$$n^2 = \epsilon_\infty + (G^2/\omega_0{}^2 - \omega^2), \quad G^2 \equiv (\epsilon_0 - \epsilon_\infty)\omega_0{}^2, \tag{22}$$

the change in n induced by a strain $\Delta\tau$ becomes

$$\Delta n = \frac{1}{2n}\left[\frac{\alpha\omega_0{}^2}{\omega_0{}^2 - \omega^2} + \frac{\beta\omega_0{}^4}{(\omega_0{}^2 - \omega^2)^2} + \gamma\right]\Delta\tau, \tag{23a}$$

where

$$\alpha \equiv \frac{1}{\omega_0{}^2}\frac{\Delta G^2}{\Delta\tau}, \qquad \beta \equiv \frac{-G^2\Delta\omega_0{}^2}{\omega_0{}^4}\frac{}{\Delta\tau}, \qquad \gamma \equiv \frac{\Delta\epsilon_\infty}{\Delta\tau}, \tag{23b}$$

so that the corresponding elastooptic constant p is then

$$p(\omega) = -\frac{1}{n^4(\omega)}\left[\frac{\alpha\omega_0{}^2}{\omega_0{}^2 - \omega^2} + \frac{\beta\omega_0{}^4}{(\omega_0{}^2 - \omega^2)^2} + \gamma\right]. \tag{24}$$

The frequency dependence of p induced by the lat-

tice, as contained in the first two terms on the right, is seen to be a result of the stress dependence of e_T^* and ω_0. HM's theory essentially provides a simplified prescription for calculating α and β, once the interionic potential $v(r)$ and distortion dipole moment $m(r)$ of the crystal have been specified. Evaluation of the electronic parameter γ would require analogous prescriptions for stress-induced effects on the electronic frequencies and polarizabilities. As frequencies close to the electronic gap are approached, dispersion effects analogous to the lattice-induced ones will arise.[23] Unfortunately, a useful first principles theory of these effects does not appear to be presently available. However, since we are not here concerned with electronic dispersion (which is, in fact, negligible for ir laser window materials), just a single measurement of p at frequencies below the electronic dispersion regime is all that is required to fix the value of γ. Such information is, in fact, available for many crystals of interest.[24] In other instances, one may still estimate γ from relationships between the ps and other measured quantities, such as in Eq. (21).

To make the qualitative discussion given above precise, one must properly associate the various specific p_{ij}s with strains τ_i. As suggested by their definitions, α is principally determined by the microscopic dipole moment $m(r)$, while β is determined by the interionic potential $v(r)$. Using a nearest neighbor (n.n.) approximation HM obtains for RS-type crystals the results

$$\begin{aligned}
\alpha_{11} &= (-G^2/\omega_0^2)[1 - 4r_0m''(r_0)/e_s^*] ,\\
\alpha_{12} &= (-G^2/\omega_0^2)[1 - 4m'(r_0)/e_s^* \\
&\qquad + 4m(r_0)/r_0e_s^*] ,\\
\alpha_{44} &= (4G^2/\omega_0^2)[m'(r_0) - m(r_0)/r_0]/e_s^* , \qquad (25)\\
\beta_{11} &= (-2G^2/\omega_0^4\mu)[r_0v'''(r_0)] ,\\
\beta_{12} &= \beta_{44} = (-2G^2/\omega_0^4\mu)[v''(r_0) - v'(r_0)/r_0] ,
\end{aligned}$$

where μ is the reduced mass and where α_{ij} and β_{ij} are the parameters corresponding to the three independent p_{ij}s in the present case; the primes indicate derivatives, and e_s^* is the Szigeti charge, related to e_T^* by $e_s^* = 3e_T^*/(\epsilon_\infty + 2)$. The results for the ZB structure are

$$\begin{aligned}
\alpha_{11} &= -\frac{G^2}{\omega_0^2}\left\{1 - \frac{2}{e_T^*}\left[\frac{4}{9}r_0m''(r_0) + \frac{8}{3}m'(r_0) \right.\right.\\
&\qquad \left.\left. - \frac{8}{3r_0}m(r_0)\right]\right\},\\
\alpha_{12} &= -\frac{G^2}{\omega_0^2}\left[1 - \frac{8}{9e_T^*}r_0m''(r_0)\right],\\
\alpha_{44} &= \frac{G^2}{\omega_0^2}\frac{2}{e_T^*}\left\{\frac{4}{9}r_0m''(r_0) - \frac{16}{27}\frac{r_0}{\mu\omega_0^2}\left[v''(r_0)\right.\right.\\
&\quad \left.\left. - \frac{v'(r_0)}{r_0}\right]\left[m''(r_0) - \frac{3}{r_0}m'(r_0) + \frac{3}{r_0^2}m(r_0)\right]\right\},
\end{aligned} \qquad (26)$$

$$\begin{aligned}
\beta_{11} &= -\frac{G^2}{\mu\omega_0^4}\left[\frac{4}{9}r_0v'''(r_0) + \frac{8}{3}v''(r_0) - \frac{8}{3r_0}v'(r_0)\right],\\
\beta_{12} &= -\frac{G^2}{\mu\omega_0^4}\left[\frac{4}{9}r_0v'''(r_0)\right],\\
\beta_{44} &= -\frac{G^2}{\mu\omega_0^4}\left\{\frac{4}{9}r_0v'''(r_0) - \frac{16}{27}\frac{r_0}{\mu\omega_0^2}\left[v''(r_0)\right.\right.\\
&\quad \left.\left. - \frac{1}{r_0}v'(r_0)\right]\left[v'''(r_0) - \frac{3}{r_0}v''(r_0) + \frac{3}{r_0^2}v'(r_0)\right]\right\}.
\end{aligned}$$

Clearly, once the functions v and m are specified, the calculation of the ps becomes a straightforward matter. However, except for the choice of a Born-Mayer potential for v for alkali halides [see Eq. (16)], very little is known about how properly to choose v or m. We thus settle for functions of a physically reasonable but simple form and adjust parameters with available prescriptions, such as the thermodynamic ones discussed in Born and Huang.[21] We write the moment for ionic crystals as

$$m(r) = m_0er_0\exp(-r/\rho_1) \qquad (27)$$

similar to the short-range portion of v. For semiconductors we choose a Morse potential for v and exponential for m; specifically,

$$\begin{aligned}
v(r) &= (H/4)\{\exp[-2\xi(r - r_0)] \\
&\qquad - 2\exp[-\xi(r - r_0)]\},\\
m(r) &= m_0er_0\exp[-2\xi_1(r - r_0)].
\end{aligned} \qquad (28)$$

The limitations of such models are quite apparent. Nevertheless, they do provide a reasonable starting point toward meaningful first-principles calculations of the elastooptic constants.

HM present various prescriptions for determining the parameters in v and m, which would leave one parameter undetermined in each except for the Born-Mayer v, if the above functional forms are employed. Since the choices made for the undetermined parameters in HM were for the most part arbitrary, it is doubtful that they are very accurate. For this reason, we will exploit the relation between the ps and dn/dP in order to better determine the unknown parameters.

B. *Determination of Parameters in m and v*

In order to obtain additional conditions for the determination of m and v, we note that Eq. (20) employed in conjunction with a direct comparison of Eqs. (14) and (24) yields

$$\begin{aligned}
\alpha_{11} + 2\alpha_{12} &= -3\left(1 + \frac{2}{K}\frac{1}{e_T^*}\frac{de_T^*}{dP}\right)(\epsilon_0 - \epsilon_\infty) ,\\
\beta_{11} + 2\beta_{12} &= \frac{6}{\omega_0K}\frac{d\omega_0}{dP}(\epsilon_0 - \epsilon_\infty).
\end{aligned} \qquad (29)$$

Since the αs and βs are known functionals of m and v [see Eqs. (25) and (26)], these may be employed in the

Table VI. Interionic Potential and Moment Function Parameters for Ionic Crystals

$v = \pm(e^2/r) + \lambda\exp(-r/\rho)$, $m = m_0 e r_0 \exp(-r/\rho_1)$

Material	$\lambda(10^{-8}$ erg)[a]	r_0/ρ[a]	m_0 HM	m_0 This work	r_0/ρ_1[b] This work
LiF	0.105	8.24	39.4	1.368	3.338
LiCl	0.078	7.75	54.4	2.731	2.886
LiBr	0.082	7.91	72.4	3.238	2.888
NaF	0.111	8.03	17.7	7.12×10^2	12.25
NaCl	0.147	8.57	105.1	3.196	3.771
NaBr	0.194	8.96	166.6	3.448	3.612
NaI	0.171	8.90	154.2	4.564	4.266
KF	0.194	8.85	59.8	1.432	2.526
KCl	0.363	9.69	199.3	6.159	5.393
KBr	0.393	9.85	292.2	6.512	5.135
KI	0.460	10.11	437.0	15.16	6.053
RbF	0.188	8.88	25.5	1.046	2.224
RbCl	0.346	9.67	165.8	5.651	5.515
RbBr	0.351	9.80	183.6	14.49	6.761
RbI	0.580	10.40	491.7	3.722	4.163
MgO	97.5	15.32	-1.29×10^5	1.364	1.134
CaO	367.8	16.95	-5.68×10^5	5.609	1.648
AgCl	16.0	13.76	1.14×10^4	3.257	2.599
AgBr	35.2	14.59	2.56×10^4	3.248	2.661

[a] Calculated by prescriptions of Ref. 21; applicability to MgO, CaO, AgCl, and AgBr is uncertain.

[b] HM choose $\rho_1 = \rho$.

determination of the parameters entering m and v. For the ionic case one obtains from Eqs. (16), (27), and (29)

$$\frac{1}{e_T^*}\frac{de_T^*}{dP} = -\frac{2K}{3e_s^*}\left[em_0\exp(-r_0/\rho_1)\right]\left[\left(\frac{r_0}{\rho_1}\right)^2 - 2\left(\frac{r_0}{\rho_1}\right) - 2\right], \quad (30a)$$

$$\frac{1}{\omega_0}\frac{d\omega_0}{dP} = \frac{K}{3\mu\omega_0^2}\frac{\lambda\exp(-r_0/\rho)}{r_0^2}\left[\left(\frac{r_0}{\rho}\right)^3 - 2\left(\frac{r_0}{\rho}\right)^2 - 2\left(\frac{r_0}{\rho}\right)\right]. \quad (30b)$$

For the ZB semiconductor case one obtains

$$\frac{1}{e_T^*}\frac{de_1^*}{dP} = -\frac{8K}{9}\frac{m_0 e}{e_T^*}\left[2\xi_1^2 r_0^2 - 2\xi_1 r_0 - 1\right], \quad (31a)$$

$$\frac{1}{\omega_0}\frac{d\omega_0}{dP} = \frac{8\sqrt{3}r_0}{9\mu\omega_0^2}\left[3\xi r_0 - 2\right]. \quad (31b)$$

An additional relation obtained by HM is

$$e_s^* = e + 2[m'(r_0) + 2m(r_0)/r_0] \quad (32a)$$

for ionic crystals and

$$e_T^* = \frac{4}{3}[m'(r_0) + 2m(r_0)/r_0] \quad (32b)$$

for semiconductors. In addition, one has the standard thermodynamic relations[25] for the vs. In the ionic case v is overdetermined, with the thermodynamic relation plus Eq. (30b). In this case the thermodynamic relation is preferred, since Eq. (30b) does not include long range terms. In fact, we calculate a difference of 20% in γ_{TO} contributed by long range terms. For semiconductors, however, an extra parameter is present, so that Eq. (31b) is needed. Equations (30a) and (32a) serve to determine m for the ionics, and Eqs. (31a) and (32b) for the semiconductors.

In Tables VI and VII we list values for the parameters determined on the basis of the present prescriptions; those determined on the basis of HM are also listed for comparison. It may be observed that we predict substantially longer range ms, and, for the case of semiconductors, v, than do HM. In what follows we will present computations of the ps based on both the present and HM prescriptions and compare the results.

VII. Wavelength Dependence of ps—Numerical Computations

In this section we present computations of the elastooptic coefficients p_{ij}, based on the theoretical models detailed in Sec. VI. We also investigate the consistency relation, Eq. (20), between dn/dP and the ps within the various models. We carry out computations both for parameters taken according to

Table VII. Interionic Potential and Moment Function Parameters for Semiconductors

$v = (H/4)\{\exp[-2\xi(r - r_0)] - 2\exp[-\xi(r - r_0)]\}$, $m = m_0 e r_0 \exp[-2\xi_1(r - r_0)]$

Material	H (10^{-10} erg) HM	H (10^{-10} erg) This work	ξ (Å^{-1}) HM	ξ (Å^{-1}) This work	$-m_0$ HM	$-m_0$ This work	ξ_1 (Å^{-1})[a] This work
GaP	0.0711	0.252	2.02	1.072	0.20	1.487	0.642
GaAs	0.0669	0.162	1.95	1.249	0.22	2.442	0.544
GaSb	0.0665	0.167	1.80	1.132	0.21	2.133	0.520
AlSb	0.0680	0.187	1.79	1.079	0.23	1.953	0.542
ZnS	0.0567	0.136	2.03	1.311	0.21	3.755	0.518
ZnSe	0.0532	0.141	1.94	1.188	0.20	3.533	0.495
ZnTe	0.0566	0.169	1.81	1.039	0.20	4.693	0.441
CdTe	0.0572	—	1.70	—	0.23	—	—

[a] HM choose $\xi_1 = \xi$.

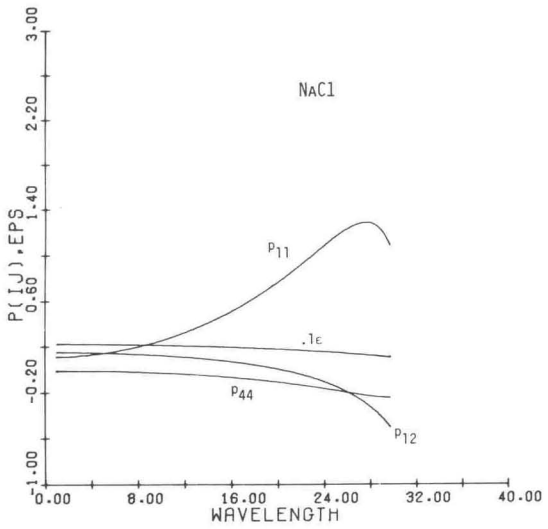

Fig. 4. Elastooptic parameters p_{ij} and dielectric constant ϵ as functions of wavelength (μm) for NaCl, calculated using HM's prescriptions.

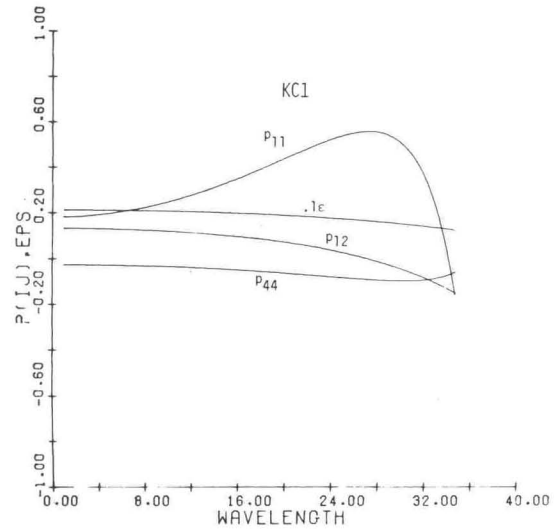

Fig. 5. Same as Fig. 4, but for KCl.

HM's prescriptions and for those computed on the basis of Eq. (29) of the present work.

The elastooptic coefficients p_{ij} and the dielectric constant ϵ are plotted in Figs. 4–6 as functions of wavelength using HM parameters, for a variety of typical ionic and semiconducting materials. For cases where the electronic contributions are unavailable, these are taken to be zero, and just the lattice contribution is plotted. The coefficients α, β, and γ for this case are listed in Tables VIII and IX. Values of the ps at various wavelengths of interest are tabulated in Tables X and XI. The analogous quantities, calculated for various materials on the basis of the prescriptions of the present work, are displayed in Figs. 7–9 and Tables XII–XV.

The lattice contributions to the ps in the present method have been calculated by employing various consistency relations between the parameters in the ps and dn/dP. Thus it is expected that the lattice contributions to dn/dP will be very nearly the same whether calculated directly from $d\omega_0/dP$ and de^*/dP or if calculated from the ps via Eq. (20). The electronic contributions may be different due to inconsistencies between $(dn/dP)_e$ and the p^es, which leads to a constant displacement between curves calculated in the two methods. Employing p_{ij}s calculated with HM's parameters leads to still another curve for dn/dP. Results calculated according to these three methods are displayed for exemplary crystals in Fig. 10, where it is seen, as expected, that the lattice portion of dn/dP calculated from phonon data is reasonably consistent with that calculated from the ps of the present work but differs from that calculated from the HM ps.

It should be pointed out that within the present approximations there are no lattice contributions to the photoelasticity of diamond-type semiconductors, since these are not ir active ($e_T^* = 0$). Higher order lattice processes do provide a small dispersion which for our purposes is negligible. Thus, for these crystals, the p_{ij}s are determined entirely by their electronic contributions.

We now present an example where the dispersion of the ps can play a significant role in determining the properties of the material under consideration. Namely, as mentioned previously, the p_{ij}s are involved in the determination of thermally induced stresses in high power laser applications. The effect of the induced birefringence on thermal lensing of spatially nonuniform beams is contained in the thermal lensing parameters S_i^α describing the induced phase shifts accompanying lensing (see Ref. 4). We consider a circular window of a cubic diatomic crystal whose face is a {111} plane, employing results for this case due to Horrigan.[26] Also, we consider an isotropic model commonly employed in the literature which ignores crystallinity. Then, explicitly

(a) {111} Plane:

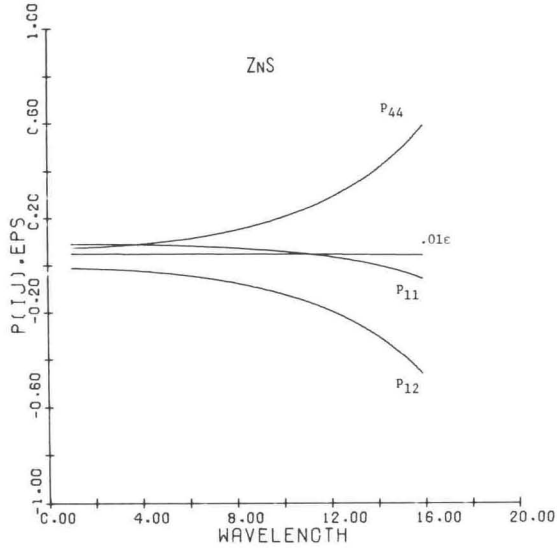

Fig. 6. Same as Fig. 4, but for ZnS.

Table VIII. Elastooptic Parameters of Ionic Crystals (HM Values)

$$p_{ij} = -n^{-4}\left(\frac{\alpha_{ij}}{1-\omega^2/\omega_0^2} + \frac{\beta_{ij}}{(1-\omega^2/\omega_0^2)^2} + \gamma_{ij}\right)$$

Crystal	α_{11}	β_{11}	γ_{11}	α_{12}	β_{12}	γ_{12}	α_{44}	β_{44}	γ_{44}
LiF	15.56	187.93	−0.067	−9.97	−25.58	−0.464	−3.06	−25.58	0.230
LiCl	62.54	351.35	—	−19.77	−51.21	—	−10.47	−51.21	—
LiBr	89.46	418.74	—	−24.21	−59.82	—	−14.21	−59.82	—
NaF	2.07	65.22	−0.144	−4.17	−9.15	−0.463	−0.77	−9.15	0.058
NaCl	25.04	72.22	−0.554	−7.38	−9.40	−0.775	−3.73	−9.40	0.050
NaBr	33.75	80.98	−0.998	−8.46	−10.06	−1.244	−4.66	−10.06	0.024
NaI	30.92	73.44	—	−8.02	−9.18	—	−4.33	−9.18	—
KF	8.45	80.60	−0.593	−5.57	−10.17	−0.457	−1.57	−10.17	0.061
KCl	12.86	50.76	−0.825	−4.49	−5.78	−0.608	−1.77	−5.78	0.118
KBr	17.71	47.42	−1.274	−4.87	−5.30	−1.011	−2.27	−5.30	0.122
KI	22.30	41.43	−1.530	−5.09	−4.51	−1.232	−2.69	−4.51	0.095
RbF	0.94	96.45	—	−5.30	−12.13	—	−0.70	−12.13	—
RbCl	9.84	49.68	−1.393	−4.13	−5.67	−0.833	−1.43	−5.67	0.203
RbBr	9.59	42.97	−1.550	−3.97	−4.84	−0.979	−1.37	−4.84	0.180
RbI	22.01	50.09	−1.771	−5.52	−5.28	−1.129	−2.62	−5.28	0.162
MgO	−107.73	254.07	2.72	0.39	−17.66	0.629	7.03	−17.66	0.965
CaO	−136.53	363.12	—	0.29	−22.73	—	8.06	−22.73	—
AgCl	100.72	575.07	—	−16.81	−44.91	—	−8.51	−44.91	—
AgBr	114.62	593.54	—	−17.52	−43.50	—	−9.02	−43.50	—

Table IX. Elastooptic Parameters of Semiconductors (HM Values)

$$p_{ij} = -n^{-4}\left(\frac{\alpha_{ij}}{1-\omega^2/\omega_0^2} + \frac{\beta_{ij}}{(1-\omega^2/\omega_0^2)^2} + \gamma_{ij}\right)$$

Crystal	α_{11}	β_{11}	γ_{11}	α_{12}	β_{12}	γ_{12}	α_{44}	β_{44}	γ_{44}
GaP	−5.92	5.36	10.802	−15.55	9.24	5.859	7.19	−3.36	5.299
GaAs	−6.89	6.01	19.590	−18.08	10.36	16.610	7.50	−3.28	8.559
ZnS	−11.37	15.15	−2.278	−29.83	26.11	0.241	32.88	−26.38	−1.865
ZnSe	−10.68	12.56	—	−28.02	21.65	—	24.34	−16.77	—
CdTe	−10.68	13.34	—	−28.02	22.99	—	27.39	−20.33	—
Si	0	0	−11.7	0	0	−1.44	0	0	−10.8
Ge	0	0	−69.1	0	0	−60.2	0	0	−32.0

Table X. Elastooptic Constants of Ionic Crystals at Various Wavelengths (HM Values)

Crystal	Electronic Values			3.9 μm			10.6 μm		
	p_{11}	p_{12}	p_{44}	p_{11}	p_{12}	p_{44}	p_{11}	p_{12}	p_{44}
LiF	0.020	0.128	−0.064	0.077	0.100	−0.083	−0.594	−0.299	−0.199
LiCl[a]	—	—	—	0.047	−0.015	−0.008	0.384	−0.142	−0.067
LiBr[a]	—	—	—	0.033	−0.009	−0.005	0.266	−0.077	−0.043
NaF	0.050	0.160	−0.020	0.057	0.153	−0.023	−0.020	0.100	−0.031
NaCl	0.110	0.153	−0.010	0.131	0.149	−0.013	0.277	0.122	−0.035
NaBr	0.148	0.184	−0.004	0.162	0.182	−0.005	0.262	0.170	−0.018
NaI[a]	—	—	—	0.008	−0.002	−0.001	0.057	−0.016	−0.008
KF	0.264	0.203	−0.027	0.291	0.195	−0.032	0.455	0.135	−0.061
KCl	0.182	0.134	−0.026	0.192	0.132	−0.028	0.257	0.119	−0.037
KBr	0.241	0.191	−0.023	0.248	0.190	−0.024	0.297	0.184	−0.030
KI	0.210	0.169	−0.013	0.215	0.168	−0.014	0.250	0.164	−0.018
RbCl	0.288	0.172	−0.042	0.293	0.171	−0.043	0.329	0.165	−0.048
RbBr	0.293	0.185	−0.034	0.296	0.185	−0.034	0.314	0.182	−0.037
RbI	0.262	0.167	−0.024	0.265	0.167	−0.024	0.286	0.164	−0.027

[a] Electronic values not available; ps computed with $\gamma = 0$.

Table XI. Elastooptic Constants of Semiconductors at Various Wavelengths (HM Values)

Crystal	Electronic values			3.9 μm			10.6 μm		
	p_{11}	p_{12}	p_{44}	p_{11}	p_{12}	p_{44}	p_{11}	p_{12}	p_{44}
GaP	−0.151	−0.082	−0.074	−0.154	−0.087	−0.072	−0.181	−0.134	−0.059
GaAs	−0.165	−0.140	−0.072	−0.166	−0.142	−0.072	−0.176	−0.160	−0.069
ZnS	0.091	−0.010	0.075	0.087	−0.024	0.091	0.051	−0.142	0.228
ZnSe[a]	—	—	—	−0.002	−0.005	0.004	−0.016	−0.041	0.035
CdTe[a]	—	—	—	−0.001	−0.002	0.002	−0.005	−0.014	0.012

[a] Electronic values not available; Ps computed with $\gamma = 0$.

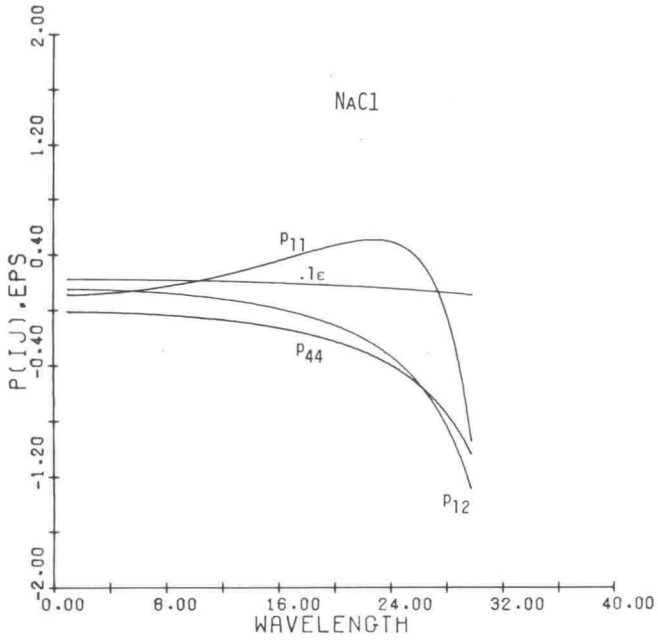

Fig. 7. Elastooptic parameters p_{ij} and dielectric constant ϵ as functions of wavelength (μm) for NaCl, calculated using prescriptions of the present work.

$$S_1^{\rho} = \partial n/\partial T + \frac{1}{12}\bar{\alpha}n^3[(1 - 4\nu)p_{11} + (5 - 8\nu)p_{12} - 2(1 + 2\nu)p_{44}] + \bar{\alpha}(1 + \nu)(n - 1),$$

$$S_1^{\theta} = \partial n/\partial T + \frac{1}{12}\bar{\alpha}n^3[(3 - 2\nu)p_{11} + (3 - 10\nu)p_{12} + 2(3 + 2\nu)p_{44}] + \bar{\alpha}(1 + \nu)(n - 1), \quad (33)$$

$$S_2^{\rho} = \frac{1}{24}\bar{\alpha}n^3(1 + \nu)(p_{11} - p_{12} + 4p_{44}).$$

(b) Isotropic Model:

$$S_1^{\rho} = \partial n/\partial T + \frac{1}{2}\bar{\alpha}n^3[(1 - \nu)p_{12} - \nu p_{11}] + \bar{\alpha}(1 + \nu)(n - 1),$$

$$S_1^{\theta} = \partial n/\partial T + \frac{1}{2}\bar{\alpha}n^3(p_{11} - 2\nu p_{12}) + \bar{\alpha}(1 + \nu)(n - 1), \quad (34)$$

$$S_2^{\rho} = \frac{1}{8}\bar{\alpha}n^3(1 + \nu)(p_{11} - p_{12}),$$

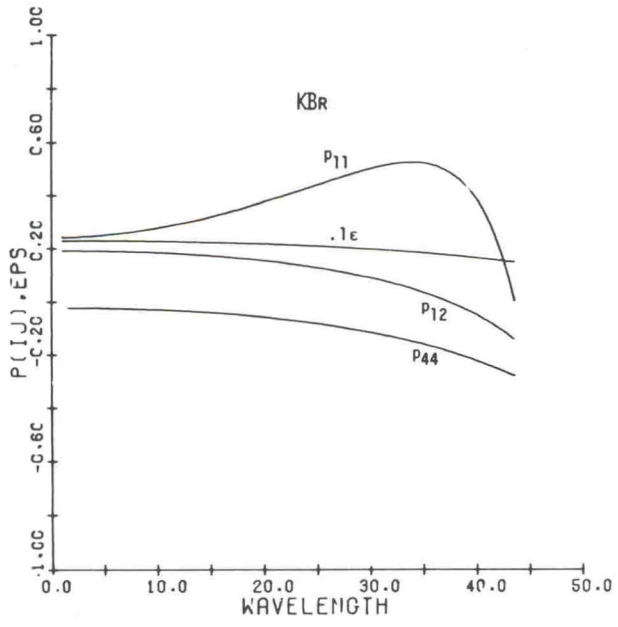

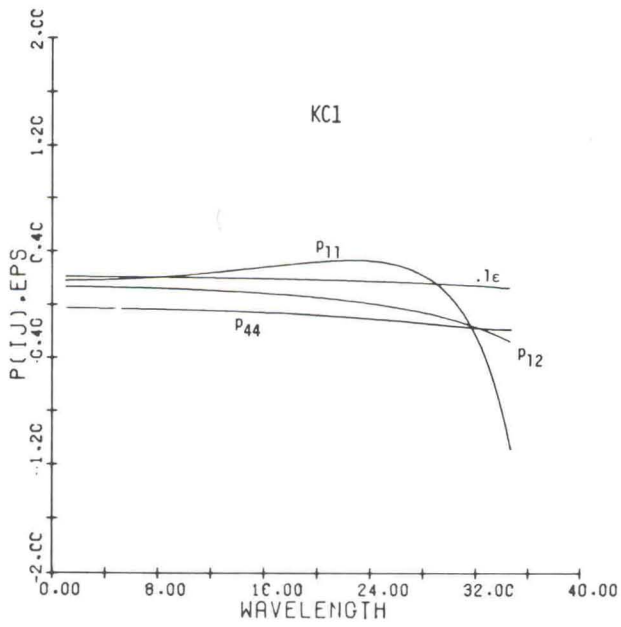

Fig. 8. Same as Fig. 7, but for KCl and KBr.

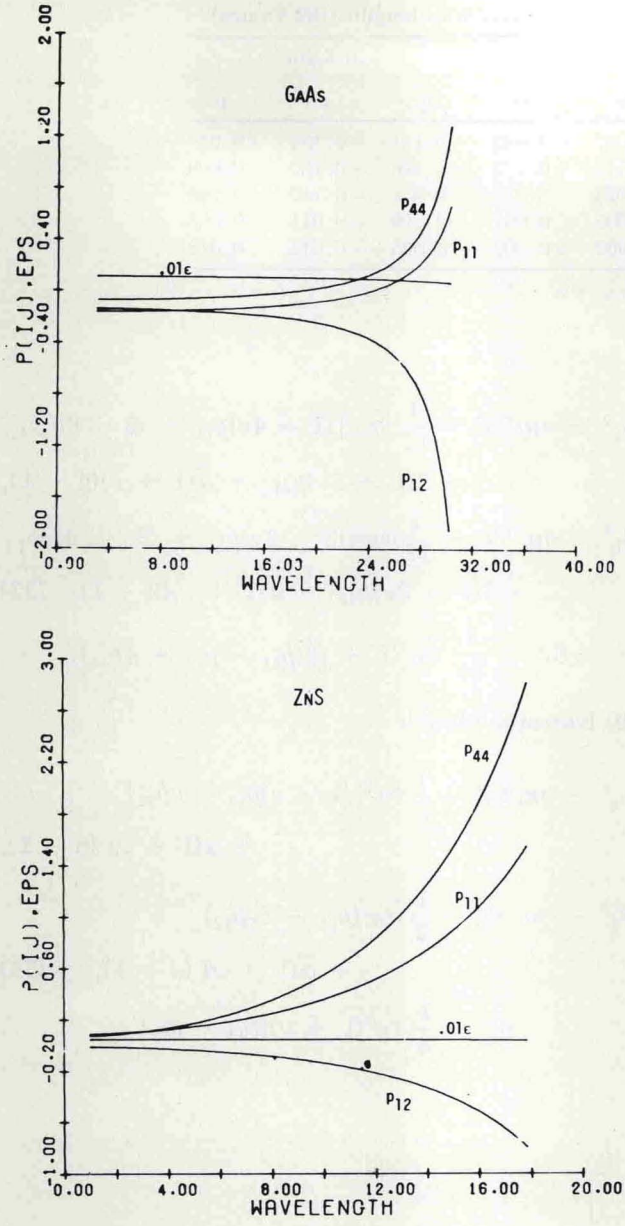

Fig. 9. Same as Fig. 7, but for GaAs and ZnS.

where $\partial n/\partial T$ is the temperature derivative of the refractive index at zero stress, $\bar{\alpha}$ the linear thermal expansion coefficient, and ν Poisson's ratio. We note that $\nu = -\frac{2}{3}(s_{11} + 2s_{12} - \frac{1}{2}s_{44})/(s_{11} + s_{12} + s_{12} + \frac{1}{2}s_{44})$ for case (a), and $\nu = -s_{12}/s_{11}$ for case (b), where the s_{ij}s are elastic constants. The dispersions of the S_i^{α} are illustrated for KCl in Fig. 11 employing HM's parameters. The influence of stress-induced birefringence is conveniently described in terms of departure of S_2^{ρ}/S_1^{ρ} from zero (or, equivalently, a departure of $S_1^{\theta}/S_1^{\rho} = 1 + 4S_2^{\rho}/S_1^{\rho}$ from unity). Values for this ratio at two different wavelengths, for the two cases mentioned above, are listed in Table XVI.

VIII. Summary and Conclusions

We have presented a theory of stress and pressure dependence of refraction in transparent solids, employing an oscillator model for the lattice and electronic responses of the material. In essence, the present approach boils down to requiring the change in the bandgap, lattice resonance frequency, and transverse effective charge as functions of pressure and stress. We have shown that the empirical pseudopotential method is useful for obtaining the pressure dependence of the gap for semiconductors, while application of the Phillips-Van Vechten approach is useful for ionic crystals. The lattice quantities are obtained either experimentally or from semiphenomenological expressions. The wavelength dependence of photoelasticity is calculated within the Humphreys-Maradudin framework but employing parameters different from these authors. The results of the various computations appear to be in reasonable agreement with existing experimental data where available, but there are virtually no useful data for stress and pressure effects on refraction in the ir. It will be important for ir applications if the latter situation can be remedied in the near future.

The magnitude of dn/dP is found to be of the order of 10^{-6}/atmosphere for the crystals investigated here. Elastooptic constants very roughly are of the order of the inverse dielectric constant. For the best 10.6-μm window materials from a lattice absorption point of

Table XII. Elastooptic Parameters of Ionic Crystals (This Work)

Crystal	α_{11}	β_{11}	α_{12}	β_{12}	α_{44}	β_{44}
LiF	10.29	187.93	−13.60	−25.58	−6.69	−25.58
LiCl	55.35	351.35	−39.46	−51.21	−30.16	−51.21
LiBr	78.58	418.74	−51.37	−59.82	−41.37	−59.82
NaF	4.09	65.22	−4.06	−9.15	−0.66	−9.15
NaCl	16.94	72.22	−10.55	−9.40	−6.90	−9.40
NaBr	22.56	80.98	−13.11	−10.06	−9.31	−10.06
NaI	20.52	73.44	−10.69	−9.18	−7.00	−9.18
KF	9.30	80.60	−11.37	−10.17	−7.37	−10.17
KCl	8.22	50.76	−5.12	−5.78	−2.40	−5.78
KBr	11.21	47.42	−5.81	−5.30	−3.21	−5.30
KI	15.32	41.43	−5.81	−4.51	−3.41	−4.51
RbCl	6.20	49.68	−4.61	−5.67	−1.91	−5.67
RbBr	6.91	42.97	−4.22	−4.84	−1.62	−4.84
RbI	12.59	50.09	−7.51	−5.28	−4.61	−5.28

Table XIII. Elastooptic Parameters of Semiconductors (This Work)

Crystal	α_{11}	β_{11}	α_{12}	β_{12}	α_{44}	β_{44}
ZnS	71.88	5.89	−33.54	16.86	107.56	−20.25
ZnSe	67.28	4.17	−31.44	13.26	85.60	−12.85
GaP	15.00	1.03	−11.94	4.91	16.49	−2.81
GaAs	27.92	2.30	−16.26	6.65	25.28	−2.95

view ($\omega_{10.6\ \mu m} \gg \omega_0$), the wavelength variation in dn/dP is fairly small, amounting to just a few percent in going from the visible to 10.6 μm. For the elastooptic constants, however, the variations are substantially greater and may be a factor of 2 or so in some cases in going from the visible to 10.6 μm. The relative size of the lattice contributions is greater for the more highly ionic materials and, in general, increases

Table XIV. Elastooptic Constants of Ionic Crystals at Various Wavelengths (This Work)

Crystal	Electronic Values			3.9 μm			10.6 μm		
	p_{11}	p_{12}	p_{44}	p_{11}	p_{12}	p_{44}	p_{11}	p_{12}	p_{44}
LiF	0.020	0.128	−0.064	0.055	0.085	−0.099	−1.116	−0.660	−0.559
LiCl[a]	—	—	—	0.041	−0.031	−0.023	0.323	−0.300	−0.224
LiBr[a]	—	—	—	0.029	−0.019	−0.015	0.228	−0.170	−0.136
NaF	0.050	0.160	−0.020	0.063	0.153	−0.023	0.046	0.104	−0.027
NaCl	0.110	0.153	−0.010	0.125	0.147	−0.016	0.221	0.100	−0.056
NaBr	0.148	0.184	−0.004	0.158	0.180	−0.007	0.225	0.154	−0.033
NaI[a]	—	—	—	0.005	−0.003	−0.002	0.038	−0.020	−0.013
KF	0.264	0.203	−0.027	0.294	0.181	−0.046	0.475	−0.003	−0.200
KCl	0.182	0.134	−0.026	0.188	0.132	−0.028	0.232	0.116	−0.040
KBr	0.241	0.191	−0.023	0.245	0.190	−0.024	0.280	0.181	−0.032
KI	0.210	0.169	−0.013	0.214	0.168	−0.014	0.238	0.163	−0.019
RbCl	0.288	0.172	−0.042	0.292	0.171	−0.043	0.317	0.164	−0.050
RbBr	0.293	0.185	−0.034	0.295	0.185	−0.034	0.310	0.182	−0.037
RbI	0.262	0.167	−0.024	0.264	0.166	−0.025	0.278	0.163	−0.028

[a] Electronic values not available; ps computed with $\gamma = 0$.

Table XV. Elastooptic Constants of Semiconductors at Various Wavelengths (This Work)

Crystal	Electronic Values			3.9 μm			10.6 μm		
	p_{11}	p_{12}	p_{44}	p_{11}	p_{12}	p_{44}	p_{11}	p_{12}	p_{44}
ZnS	0.091	−0.010	0.075	0.125	−0.025	0.124	0.392	−0.153	0.528
ZnSe[a]	—	—	—	0.012	−0.006	0.015	0.096	−0.046	0.124
GaP	−0.151	−0.082	−0.074	−0.148	−0.086	−0.070	−0.123	−0.123	−0.034
GaAs	−0.165	−0.140	−0.072	−0.163	−0.142	−0.070	−0.150	−0.158	−0.055

[a] Electronic value not available; ps computed with $\gamma = 0$.

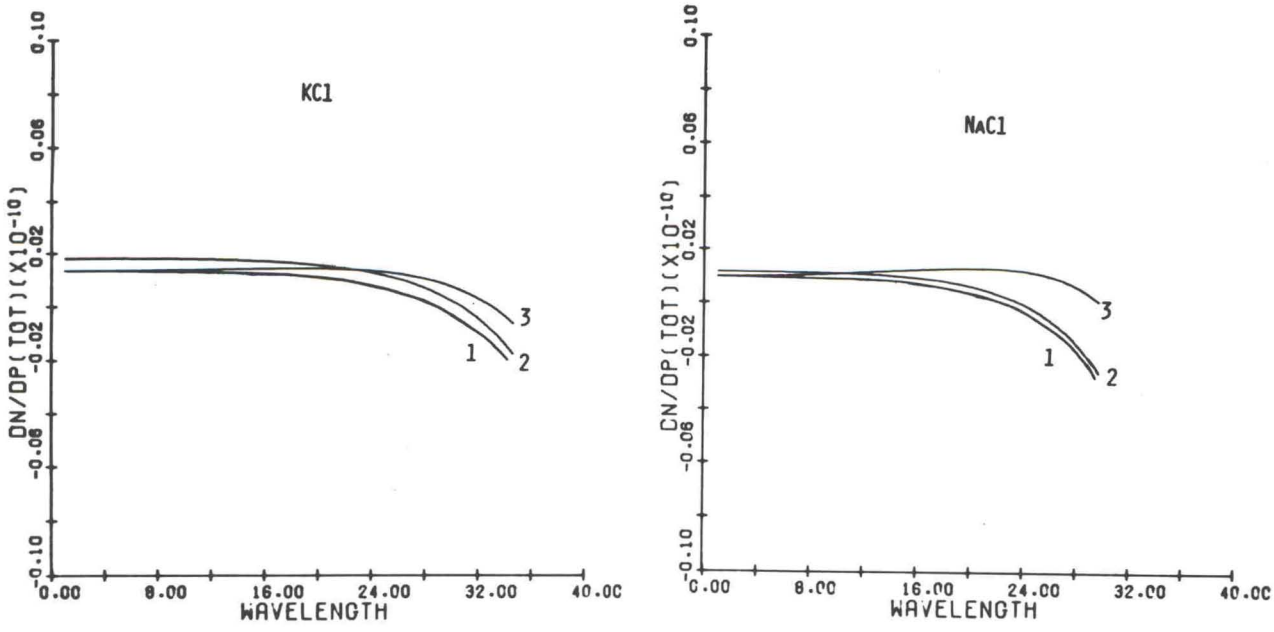

Fig. 10. Comparison of dn/dPs vs wavelength (μm) as calculated by different methods; 1 is from ps of this work; 2 is directly as in Sec. V; and 3 is from ps of HM.

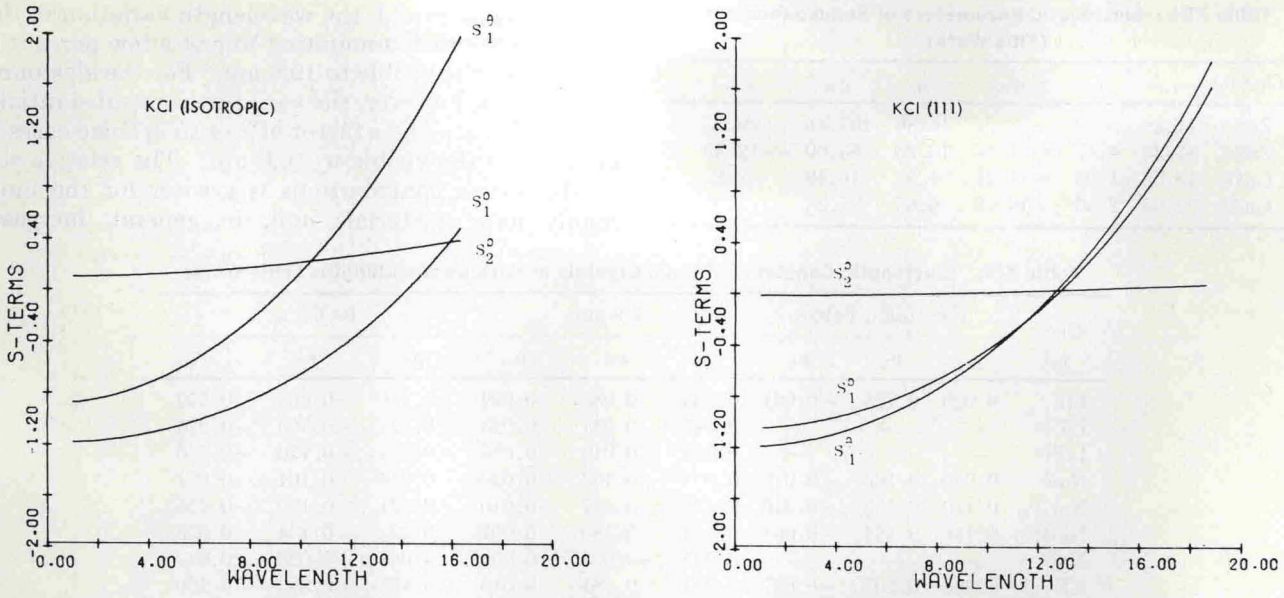

Fig. 11. Thermal lensing parameters S_i^{α} (K^{-1}) as functions of wavelength (μm) for KCl for the two models described in the text.

Table XVI. Thermal Lensing Parameters at 1.0 μm and 10.6 μm

	S_2^p/S_1^p			
	Isotropic		{111} Plane	
Crystal	10.6 μm	1.0 μm	10.6 μm	1.0 μm
KCl	−0.354	−0.065	0.014	0.034
KBr	−4.389	−0.221	0.194	0.068
NaCl	0.273	0.372	0.009	0.246
GaAs	−0.003	−0.004	−0.015	−0.016
Si	0.006	0.006	0.010	0.010
Ge	0.006	0.006	0.029	0.029

among the materials investigated in going from IV–IVs to III–Vs to II–VIs to I–VIIs. The quantitative reliability of the predicted elastooptic constants is uncertain, but the general trends exhibited are believed to be accurate.

The present calculations provide a basis for selection of materials with small stress and pressure effects on refraction. On the other hand, once a material has been chosen for a particular application, they allow for a prediction of the response under pressure or stress. It is hoped that further experimental data will become available, especially in the ir, to provide a test for the theory.

The work of Yet-Ful Tsay and S. S. Mitra is supported by Air Force Cambridge Research Laboratories (AFSC) under Contract F19628-72-C-0286.

References

1. M. Born and E. Wolf, *Principles of Optics* (Macmillan, New York, 1964); J. F. Nye, *Physical Properties of Crystals* (Oxford U.P., London, 1964).
2. See, for example, *Proceedings of 1972 Conf. on High-Power IR Laser Window Materials,* C. A. Pitha, Ed. (AFCRL-TR-73-0372, AFCRL, Bedford, Mass., 1973); *Proceedings of the Electronic Materials Conference,* published in J. Elec. Mater. **2** (February and May issues in 1973).
3. See, for example, M. Sparks and M. Cottis, J. Appl. Phys. **44,** 787 (1973).
4. M. Sparks, J. Appl. Phys. **42,** 5029 (1971); B. Bendow and P. D. Gianino, J. Elec. Mater. **2,** 87 (1973); Appl. Phys. **2,** 1, 71 (1973).
5. J. F. Nye, Ref. 1; and D. A. Pinnow in *Laser Handbook,* F. T. Arecchi and E. O. Schulz-Dubois, Eds. (North-Holland, Amsterdam, 1972), Vol. 1.
6. L. B. Humphreys and A. A. Maradudin, Phys. Rev. **B6,** 3868 (1972).
7. A preliminary account of the aplication of the HM theory for calculating the *ps* was given by B. Bendow and P. D. Gianino in *Laser Induced Damage in Optical Materials, 1973,* NBS Spec. Publ. 387 (U.S. Govt. Printing Office, Washington, D.C., 1973).
8. Y. F. Tsay, B. Bendow, and S. S. Mitra, Phys. Rev. **B8,** 2688 (1973).
9. See, for example, J. M. Ziman, *Principles of the Theory of Solids* (Cambridge U.P., Cambridge, 1967).
10. M. L. Cohen and V. Heine in *Solid State Physics,* F. Seitz and D. Turnbull, Eds. (Academic Press, New York, 1970), Vol. 24;

W. A. Harrison, *Pseudopotentials in the Theory of Metals* (Benjamin, New York, 1966).
11. D. L. Camphausen, G. Connell, and W. Paul, Phys. Rev. Lett. **26,** 184 (1971).
12. J. A. Van Vechten, Phys. Rev. **182,** 891 (1969).
13. Y. F. Tsay, S. S. Mitra, and B. Bendow, Phys. Rev. B (in press).
14. P. Melz, J. Phys. Chem. Sol. **32,** 209 (1971).
15. M. L. Cohen and V. Heine, Ref. 10.
16. D. Brust and L. Liu, Phys. Rev. **154,** 647 (1967).
(1966).
18. Experimental values cited in Ref. 11.
19. S. H. Wemple and J. DiDomenico, Phys. Rev. **B3,** 1338 (1971).
20. J. C. Phillips, Rev. Mod. Phys. **42,** 317 (1970).
21. M. Born and K. Huang, *Dynamical Theory of Crystal Lattices* (Oxford U.P., London, 1954).
22. S. S. Mitra in *Optical Proterties of Solids,* S. Nudelman and S. S. Mitra, Eds. (Plenum, New York, 1969).
23. S. H. Wemple and M. DiDomenico, Phys. Rev. **B1,** 193 (1970).
24. See, for example, D. A. Pinnow, Ref. 5; C. S. Sahagian and C. A. Pitha, *Compendium on High Power IR Laser Window Materials* (AFCRL-72-0170, AFCRL, Bedford, Mass., 1972).
25. Ref. 21, Secs. 3 and 9.
26. F. Horrigan, Raytheon Corp.; private communication.